UNIVERSITY OF CALIFORNIA, SAN DIEGO

Design and Implementation of an Adaptive Underwater Acoustic Modem and Test Platform

A Thesis submitted in partial satisfaction of the requirements for the degree
Master of Science

in

Computer Science

by

Jennifer Trezzo

Committee in charge:

Ryan Kastner, Chair
Joseph Pasquale
Curt Schurgers
Alex Snoeren

2013

The Thesis of Jennifer Trezzo is approved, and it is acceptable in quality and form for publication on microfilm and electronically:

_____

_____

_____

_____

Chair

University of California, San Diego

2013

TABLE OF CONTENTS

LIST OF FIGURES

LIST OF TABLES

ACKNOWLEDGEMENTS

I am extremely thankful for all the encouragement and support I have received during my time as a Master's student at the University of California, San Diego (UCSD). In this section I would like to take the opportunity to individually thank some of the people and organizations that have helped me get to where I am now.

First, I would like to thank Lingjuan (Nancy) Wu for being such a great colleague. We did a lot of simulation and ocean testing together and had fun hanging hydrophones off the Scripps Pier and doing testing by the pool in the beautiful San Diego sunshine. After her time at UCSD was finished, I missed her help and cheery personality around the office. I hope she continues to enjoy her life back in China.

Professor Ryan Kastner has been a great advisor over the past couple of years. He introduced me to the underwater modem project and helped me shape the project into an interesting research endeavor. He also encouraged me to apply for the NSF Graduate Research Fellowship Program, and with his help I was able to put together a competitive research proposal and application that led me to be selected for the fellowship.

Dr. Diba Mirza dedicated her time to this project as a Post Doctoral Scholar through countless weekly meetings. I truly value her advice and assistance throughout the entire process. I wish her the best with her newborn son, Aman.

Without the hard work and assistance of Dr. Bridget Benson, my research would not have come together as it did today. Her PhD research provided a base modem platform that I was able to enhance in order to realize my goal of designing an adaptable underwater acoustic modem. Her friendship over the years has also meant a lot to me.

My colleagues in Professor Kastner's research group have also provided me with support over the past couple of years. I would like to especially thank Magnus Delight, Janarbek Matai, and Perry Naughtun.

I am also very grateful to my committee members, Joseph Pasquale, Alex Snoeren, and Curt Schurgers, for taking the time to review my thesis.

Last but not least, I am so lucky to have the support of my family and friends.

Thanks to my mom and dad for giving me such great guidance throughout my entire life, and to my older brother Chris for reminding me that whatever stress or challenge I am currently facing, he went through the same thing 3 years ago. I am also so thankful for the love and support from my significant other, Ali, who is always there for me and makes me a better person every day.

The text of Chapter 4.2 is, in part, based on the material as it appears in "Designing an Adaptive Acoustic Modem for Underwater Sensor Networks", IEEE Embedded Systems Letters, vol. 3, issue 3, December 2011. The thesis author was a co-primary researcher and author (with Lingjuan Wu). The other co-authors listed on this publication [1] directed and supervised the research which forms the basis for Chapter 4.2.

This material is based upon work supported by the National Science Foundation Graduate Research Fellowship under Grant No. (DGE-1144086).

ABSTRACT OF THE THESIS

Design and Implementation of an Adaptive Underwater Acoustic Modem and Test Platform

by

Jennifer Trezzo

Master of Science in Computer Science

University of California, San Diego, 2013

Ryan Kastner, Chair

Underwater wireless sensor networks are crucial in understanding certain phenomena that take place within our vast oceans. They can be used as an integral tool in countless environmental monitoring applications like understanding the growth and spread of algal blooms and monitoring the health of coral reefs. These networks often rely on acoustic communication, which poses a number of challenges for reliable data transmission. Three of these key challenges are high power consumption when transmitting, frequency selective fading, and high variability in the communication channel over time due to factors like multipath delay spread, doppler shift, and noise interference due to low SNRs. Current modems are traditionally configured for specific environments and must withstand the worst anticipated channel conditions. This tendency limits potential performance of the modem when the channel improves. This thesis introduces the design of a low cost underwater acoustic modem that can measure the underwater communication channel and adapt its bit rate and modulation scheme to maintain re-

liable data transmission while optimizing data rates and effectively minimizing power consumption.

Chapter 1.

Introduction

Every day oceanographers and marine biologists are reminded how much still remains unknown about our oceans and the phenomena that take place within them. With the encroaching impact of environmental changes, namely global warming, it becomes more and more important that we can understand these phenomena and do everything in our power to preserve the overwhelming diversity of marine life. The first step in growing our understanding is to equip ourselves with the necessary tools to observe and study the underwater environment.

A subset of these tools involve the use of underwater sensor networks in order to propagate data throughout the observed area, oftentimes reaching a surface sink node or base station for further processing. Previously, sensor networks were connected by physical cables, which limited placement of sensors and had the potential to cause damage to fragile environments like coral reefs. Therefore, one crucial step forward in underwater sensor networks is the use of wireless communication.

Unfortunately, underwater wireless communication is plagued with many challenges. One of the most prevalent issues is frequency selective fading in the underwater environment. This issue causes certain frequencies to attenuate at a faster rate than others. As a result, radio frequencies tend to suffer from high attenuation over very short distances. Underwater wireless communication over distances greater than a few feet

is therefore restricted to the acoustic range. In addition, the acoustic communication channel is highly variable due to the effects of variables like multipath delay spread, doppler shift, and SNR. The channel also varies across water columns where there are significant differences in temperature and salinity. Consequently, reliable communication in reverberant shallow waters over different directional planes requires robustness to a wide variety of channel conditions.

Current off the shelf underwater acoustic modems are expensive and often times tailored to a specific application. This one-time customization is not ideal for dense sensor networks in highly variable shallow water environments. Unfortunately, many of the phenomena that researchers are interested in observing, like the health of coral reefs, oil spill expansion, and the dynamics of planktonic communities, require exactly this type of dense monitoring, often times in shallow waters. For this reason, Principle Investigators, Jules Jaffe and Peter Franks from the SCRIPPS Institution of Oceanography (SIO) are developing a system made up of autonomous buoyancy-controlled subsurface floats with sensors for data collection, as pictured in Figure 1.1 [2]. These floats are designed to act as sensor nodes in an ad-hoc network that can relay data to surface stations for analysis. The goal of this system is to gather ocean data with high temporal and spatial resolution in a cost effective manner. Underwater wireless sensor networks, like this one, are in need of a low cost acoustic modem that can function reliably in an extremely dynamic environment at short ranges, typically 100s of meters.

The major contribution of this thesis is the design of a low cost adaptive underwater acoustic modem intended for applications like the SIO autonomous underwater drifting sensor network. This modem is intended to measure the underwater acoustic communication channel and adapt its modulation scheme and bit rate in order to ensure power efficient and robust communication.

This thesis is outlined as follows. In Chapter 2, the challenges of underwater acoustic communication are discussed, followed by a related works section in Chapter 3. Chapter 4 presents the proposed adaptable modem at the system level, and Chapter 5 includes a description of the implemented design and its test platform. The thesis

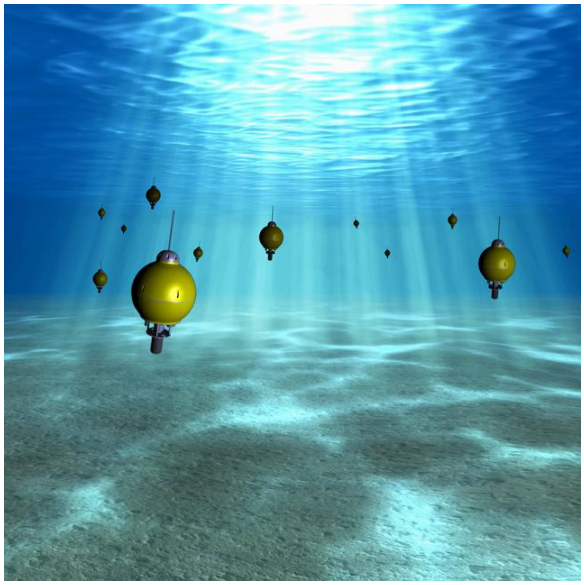

Figure 1.1: Autonomous Underwater Drifting Sensor Network [2]

concludes in Chapter 6.

Chapter 2.

Underwater Acoustic Communication

Though the challenges in the underwater communication channel are similar in nature to those in the terrestrial RF channel, they tend to be a bit more difficult to mitigate. This chapter describes the characteristics of the underwater acoustic environment along with the challenges those characteristics present. The chapter then goes into a discussion of different modulation schemes that are commonly used and how these modulation schemes hold up in this communication environment.

2.1. Channel Characteristics

Several physical layer wireless communication techniques including optical, radio frequency, and acoustic signals have been considered for short-range, dense underwater wireless sensor networks [3]. Optical signals perform poorly underwater due to scattering caused by high particulate matter in the ocean as well as the need for precise alignment between the sender and receiver. Radio frequency waves are electromagnetic waves in the frequency range from 300GHz to as low as 3KHz. Radio frequency waves attenuate quickly and can only travel short distances in bodies of salt water, due to the higher conductivity of salt water when compared with fresh water and air. For these reasons, most underwater wireless modems use acoustic communication [3]. The next

few paragraphs describe the various characteristics of the underwater acoustic channel and discuss how they effect communication.

Multipath delay spread: Due to reflections off of the surface and the ocean floor, a single transmission can arrive at a receiving node through multiple paths and at different times. Multipath delay spread is defined as the time between the arrival of the first and the last discernible sound waves that have traveled along these multiple paths [4]. If the multipath delay spread is too large, the received transmission can be difficult to demodulate due to inter-symbol interference.

Doppler shift: Doppler shift is caused by the movement of transmitting or receiving nodes in the network as well as by ocean swells and currents. This can have a significant effect on certain frequency-dependent modulation schemes.

Low and variable signal to noise ratio (SNR): The underwater communication channel suffers from significant ambient noise which can be attributed to four main sources; turbulence, shipping, breaking waves, and thermal noise. In addition, surface motion due to wind-driven waves specifically affects signals in the acoustic range [5]. This type of interference leads to relatively low SNRs and often times, less reliable communication.

High and variable propagation delay: One of the most defining characteristics of the underwater acoustic communication channel is high and variable propagation delay. Underwater acoustic signals travel five orders of magnitude slower than RF signals in terrestrial networks. A typical propagation speed for an acoustic transmission is approximately 0.67s/km [6]. To make matters worse, the speed of sound through water can vary significantly with changes in salinity and temperature.

Frequency selective fading: Frequency selective fading is a characteristic that has the effect of varying degrees of attenuation across different frequencies and transmission distances. For longer distances over several 10s of kilometers, the useable frequency bandwidth is typically limited to a few kHz. Short range communication needed in dense underwater sensor networks has slightly more frequency bandwidth compared to long range communication, but is still limited to 20-50 KHz [6].

High transmission power consumption: Power consumption is an important issue for underwater acoustic sensor networks because the nodes are battery powered and would ideally be deployed for several months at a time. Unlike terrestrial transceivers, underwater acoustic transceivers consume a significant amount of power when transmitting, mainly due to the physical characteristics of underwater acoustic transducers. The WHOI Micro Modem 1 transceiver consumes 50W when transmitting at distances of 2-3Km at a center frequency of 25KHz [7], and an underwater acoustic transceiver designed for short range communication at the University of California, San Diego consumes 6.9W when transmitting at a maximum distance of 350m with a center frequency of 40KHz [3]. Due to the high power consumption that occurs during transmission, adjusting the data rate of an underwater acoustic modem can have significant impact on overall power consumption through increases or decreases in total transmit time. Therefore, a majority of the focus on power consumption in the proposed modem presented in this thesis pertains to maximizing the modem's data rate while maintaining robust communication.

The characteristics described in this section present many challenges for underwater acoustic communication. In addition, mobile nodes in an ad hoc shallow water sensor network will also experience changes in the channel characteristics over time and space. For example, the communication channel across a horizontal plane is often times very different than it is across a vertical plane. This is mostly due to differences in multipath reflections as well as changes in propagation speed when the channel spans multiple water columns with varying temperatures or salinity. The channel naturally varies over time with differences in ambient noise, temperature, and ocean currents. Keeping these characteristics in mind, the next section describes how modulation schemes can be used to mitigate some of the major challenges.

2.2. Modulation Schemes

Due to the high variability of the underwater acoustic communication channel, several different modulation schemes have been used across the research community. These modulation schemes are also used to mitigate channel-deteriorating characteristics in terrestrial networks. The most commonly used modulation schemes and techniques for underwater communication are discussed in this section.

Frequency Shift Keying (FSK): Frequency Shift Keying is a non-coherent modulation scheme that can maintain reliable communication in harsh conditions. Many researchers use variations of FSK due to its robustness and its simple receiver design [8]. However, one major drawback with FSK is its slow bit rates when compared to other modulation schemes. For high data rate applications such as autonomous underwater vehicle (AUV) control and audio or video streaming, FSK is not ideal.

Phase Shift Keying (PSK): Contrastingly, PSK is a slightly more complex coherent modulation scheme. Coherent modulation schemes in general do not do well in multipath environments [8]. This can often times be counteracted with the use of a receiver array, but receiver arrays are not plausible for all applications.

Orthogonal Frequency Division Multiplexing (OFDM): OFDM is a modulation technique that divides the frequency band into different orthogonal sub-carrier frequencies. Each sub-carrier frequency can implement its own conventional modulation scheme. OFDM is very sensitive to doppler shift, but offers high data rates and can do well in environments with frequency selective fading and high multipath. Issues related to doppler shift can be mitigated with a complex receiver using non-uniform doppler compensation [9]. OFDM is therefore gaining more and more popularity as receiver technology advances.

Direct Sequence Spread Spectrum (DSSS): DSSS is a technique that spreads modulated data across a wider frequency band. This technique can be advantageous in withstanding channels with frequency selective fading and high multipath. Time guards are frequently used in DSSS to further reduce the chance of inter symbol interference.

Since DSSS is a spread spectrum technique, data is first modulated by a traditional modulation scheme, such as PSK, then the modulated signal is spread across a certain frequency band using DSSS.

The modulation schemes described in this section address a wide range of channel characteristics as a whole, but no single modulation technique is able to mitigate the effects of all channel characteristic on its own. For a highly variable environment that a mobile underwater sensor network would be exposed to, selecting an optimal modulation scheme and bit rate for robust and power efficient communication can be difficult. The next chapter describes a number of commercial and research-based modem designs that try to address the issues caused by the channel characteristics described in this chapter.

Chapter 3.

Related Work

There are several existing underwater acoustic modems that are either commercially available or developed by the research community. The modems most suited for a dense underwater sensor network deployed in shallow waters are described and compared in this chapter. This related work study is partly drawn from Dr. Bridget Benson's PhD Thesis [3]. However, updates have been made to ensure the study is as current and relevant as possible.

3.1. Commercial Modems

Table 3.1 shows a number of commercial modems that are well suited for dense shallow water sensor networks. This table compares various features of the modems. As a majority of these modems can be customized for a specific application by the manufacturer, some of the information is given in ranges. This comparison is intended to give a sense of the general capabilities of commercial modems. In the table, NS is used to represent information that was not specified by the manufacturer. The characteristics of the adaptable modem proposed in this thesis are also included in the table for comparison. The range, transmit power and receiver power are based on the characteristics of an analog transceiver and home made transducer that were designed and originally

used in Dr. Bridget Benson's PhD Thesis [3].

Some modems were excluded from this list due to issues like prohibitively large housings and undesirable transmission ranges or deployment setups. One important aspect to consider is the cost of each of the modems. A vast majority of commercial modems are typically priced upwards of a few thousand dollars, which limits the number of researchers and organizations that have the necessary funds to purchase enough modems to form a dense sensor network. This cost data was gathered from sales representatives at a number of companies that did not want to disclose specific pricing information. In order to make the use of dense underwater sensor networks more accessible, one of the goals of the proposed modem in this thesis is to offer a competitive design for a much more practical cost.

The AquaModem 1000 by Aquatec Group Limited [10] is a viable option with a sufficient range and bit rate. The AquaModem 1000 is customizable for the intended application. The modem can be set to utilize either FSK or differential PSK spread spectrum depending on the environment. The configurable settings of the AquaModem 1000 are updated according to advances in Aquatec Group Limited's Research and Development group. The most recent projects involve shallow water communications in the Baltic Sea.

The UWM2000H is the recommended modem for the target application out of the various models developed by LinkQuest [11]. This modem has a high bit rate of 17.8 kbps and a relatively low transmit power of 2 or 8 W depending on the desired transmission distance. Details of the modulation scheme are not available since the modem uses LinkQuest's proprietary Broadband Acoustic Spread Spectrum Technology. Some of the additional features of this modem include channel equalization to combat multipath, error correction coding, and automatic rate adaptation to combat varying noise conditions.

EvoLogic's most suitable model is the S2C R 48/78 [12]. A range of transmit powers leads to better application flexibility. The modem also has an optimal range and a relatively high bit rate. The modulation scheme used is a patented Sweep Spread Carrier

Table 3.1: Commercial Underwater Acoustic Modems

Company	Modem	Frequency (kHz)	Tx Power (W)	Max Range (Km)	Rx Power (W)	Modulation	Bit Rate (bps)
AquaTec	AquaModem 1000	7.5-12	20	20	0.6	FSK / DPSK-SS	300-2000
LinkQuest	UWM2000H	26.77-44.62	2 or 8	1.2	0.8	Proprietary SS	17,800
EvoLogics	S2C R 48/78	48-78	5, 8, 18 or 60	1	1.1	S2C	3,200
Tritech	Micron Data Modem	20-28	7.92	0.5	0.72	SS	40
DSPComm	AquaComm	16-30	Configurable	3	0.42	DSSS / OFDM	100 / 480
Teledyne Benthos	SMART Modem	9-14, 16-21 or 22-27	NS	2-6	NS	multiple FSK / PSK	140-15360
AquaSeNT	AquaSeNT Modem	14-20	5-20	4	0.7	OFDM	3200
UCSD	Proposed Modem	40	1.3-7.0	0.4	0.42	Adaptable	Adaptable

(S2C) technology. S2C is designed to mimic dolphin sound patterns by spreading the signal across a wide range of frequencies. This technique has proven to help counteract the effects of multipath.

Tritech's Micron Data Modem [13] was specifically designed for underwater communication in environments where space and/or power is limited. In comparison to the other modems described in this section, the Micron Data Modem has a much slower bit rate of 40 bits per second. However, the modem is intended for low data rate applications, and 40 bps may be sufficient for many of those scenarios. The modulation scheme for this modem is again based on a spread spectrum technology.

DSPComm's AquaComm [14] is fairly typical across the board. This modem is customizable with a choice of two bit rates, 100 or 480 bps. DSPComm designed this modem with size and flexibility in mind. Another customizable feature is the modulation scheme. Customers have a choice of utilizing either DSSS or OFDM.

Teledyne Benthos offers a number of acoustic modem models. The SMART Modem SM-975 [15] seems to be the best suited model for dense underwater sensor networks. It supports a number of features such as in-band acoustic recording, arbitrary waveform playback, Long Base Line (LBL) operations, and high capacity data logging. The SMART Modem device utilizes the same electronics as Teledyne Benthos' ATM-900 series modem electronics. This modem is highly customizable and therefore has a range of frequencies and bit rates. The modulation schemes used are MFSK and PSK.

Aquatic Sensor Network Technology LLC (AquaSeNT) [16] is a relatively new startup which was founded by three professors from the University of Connecticut's School of Engineering. The AquaSeNT modem was designed for use in underwater sensor networks to monitor and collect data in a variety of different applications. This is one of the few OFDM-based commercial modems. The modem proves to be relatively low power with a high bit rate of 3.2 kbps.

In summary, these commercial modems offer a wide range of underwater communication techniques that are suitable for underwater sensor networks. Although many of the modems are customizable for a specific application, few of them can offer real-

time flexibility in the field for a sensor network, like the SIO underwater drifting sensor network, that will be met with a number of different environments. In addition, the high cost of many of the modems makes them inaccessible for many research groups to use as part of a dense underwater sensor network. These two drawbacks provide motivation for a low cost adaptable modem.

3.2. Research Modems

The previous section discussed several commercially available modems for dense underwater sensor networks in shallow waters. This section will cover the latest advances in the research world. Table 3.2 shows a summary of the comparison between these research modems. In the table, NS is used to represent a non-specified value. The characteristics of the adaptable modem proposed in this thesis are also included in the table for comparison. The range is based on the characteristics of a custom analog transceiver and transducer that were designed and originally used in [3].

Table 3.2: Research Underwater Acoustic Modems
Note: The supported modulation schemes and bit rates for the proposed modem are as of yet unspecified. However, we have the intention of implementing a set of complementary modulation schemes and bit rates in order to show robustness to a wide array of scenarios.

Modem	Platform	Modulation	Bit Rate (bps)	Range (km)
WHOI Micro-Modem 2	DSP	FH-FSK / QPSK	80-5000	11
Fish Robot Modem	MCU	Binary AM	1000	0.3
Uconn Modem	DSP	OFDM	3200-6400	NS
HERMES	NS	BPSK / QPSK	16000-87000	0.12
AquaModem	DSP	AM-DSSS	133	440
Proposed Modem	FPGA	Adaptable	Adaptable	0.4

The Woods Hole Oceanographic Institute (WHOI) is very active in the underwater sensor network research area. The Micro-modem 2 [17] is their latest open source modem, designed in 2009, and intended to provide a flexible test platform for underwater acoustic communication research. The modem is implemented on a Blackfin ADSP-BF548. Some of the new features that were not on the original modem are an adaptive decision feedback equalizer and error-correction software. This modem has 3 modes; active, low-power detect, and hibernate. The modem can be configured to use either frequency-hopped FSK or PSK with a range of bit rates from 80-5000 bps. The performance of the Micro-Modem 2 was tested in the Mariana Trench [18] where reliable transmissions were possible at a rate of 200bps with ranges up to 11km.

A number of universities in South Korea in conjunction with the Korea Institute of Industrial Technology have developed a bio-inspired fish robot for use in a mobile underwater communication system [19]. This type of sensor network is intended for high mobility and real time monitoring in shallow water environments.The fish robot's acoustic communication technology was designed to be simple and robust in order to minimize the size of the modem. Due to this simplicity, the modem is implemented on a microcontroller (MCU). With this goal in mind, the modem uses non-coherent binary amplitude modulation with a time guard between symbols to reduce the effects of multipath. The modem can transmit at 1kbps with a bit error rate (BER) of less than 10^{-4} for up to 300 meters. These characteristics were observed during testing in the Han River, which is approximately 500 meters wide with a maximum depth of about 15 meters.

The University of Connecticut has designed a modem that uses OFDM [20]. Both single-input single-output (SISO) and multiple-input multiple-output (MIMO) versions of the modem have been implemented on both a fixed point and a floating point TMS320C6713 DSP board. The goal of this modem was to take advantage of potentially high data rates with OFDM and to experiment with the potential benefits of SISO and MIMO configurations. The University of Connecticut formed a startup called AquaSeNT (introduced in the Commercial Modem Section), which was based on a ver-

sion of this modem.

HERMES [21] is a high-speed, high-frequency underwater acoustic modem developed by Florida Atlantic University. The modem has two underwater communication links; a very high bit rate broadband data uplink and a low bit rate command downlink. HERMES can transmit high resolution uncompressed acoustic images at approximately 86.9 Kbps at a range of 120 m. The goal was to make the modem smaller than the original HS-HFAM modem off of which it was based and to extend the original maximum range of 100 m. This modem uses a commercial transducer developed by Jetasonics. The frequency band 260-380 Khz, which is significantly higher than most other acoustic modems. HERMES can be configured to use BPSK or QPSK with DSSS and can achieve rates from 16 to 87 Kbps uncoded, depending on packet specifications. Since the image transmissions in this application can tolerate higher BERs than traditional textual data, transmission is considered successful up to 120 m with 71.8% of packets detected and authenticated, and a 5.3% average BER. At a range of 95m, the percentage of packets detected and authenticated comes much closer to 100% and the BER decreases to a much more desirable value for non-image transmissions.

The UCSB AquaModem was designed for use in an ad hoc sensor network for eco-sensing applications. This modem uses amplitude modulated DSSS with a composite walsh/m-sequence format, as described in the modem's main publication [22]. The spread signal has 5 Khz of bandwidth for robustness to multipath and can achieve a data rate of 133 bps. The modulation algorithm also includes a time guard in order to eliminate the need for equalization. The modem is implemented on a TI F2812 fixed-point DSP with a custom amplifier and transducer. Testing shows that the maximum transmit power is approximately 12 W RMS.

The research modems described above utilize a range of platforms and modulation techniques. Some of the modems can be configured to operate with different modulation schemes, bit rates, and power levels. However, none of these modems take advantage of the benefits of adapting their modulation techniques according to the time-varying communication channel in real time. A dense underwater wireless sensor net-

work with mobile nodes can experience a wide variety of communication environments throughout its deployment period. Solutions that force the user to configure the modems to one specific environment before deploying them are limiting their performance.

Research has been performed concerning the prediction of channel characteristics by estimating the channel multiple times over certain intervals [23]. Although no current modems have incorporated this technique into their designs, this type of prediction would be useful in future versions of the proposed modem. In this thesis, the adaptive behavior of the proposed modem is based on channel estimation alone.

The next chapter presents one of the major contributions of this thesis by introducing a low power adaptable modem that can measure the channel characteristics and adapt its modulation scheme and bit rate to optimize power and data rates in real time, while ensuring the most reliable communication possible.

Chapter 4.

Proposed System

This chapter describes in detail the proposed adaptable modem for applications like the Scripps Institution of Oceanography (SIO) autonomous drifting sensor network [2]. The first section describes the entire proposed system, going into detail for the digital portion of the adaptive modem design, and the second section describes simulation and ocean testing of the conceptual design.

4.1. System Design

Figure 4.1: System Block Diagram

As shown in Figure 4.1, the system is made up of an underwater acoustic transducer, an analog transceiver, and the digital portion of the adaptable modem. Typically, transducers tend to be the most expensive component of an underwater acoustic modem. In order to mitigate this cost, the transducer that the original UCSD modem was

intended for is an in-house custom transducer consisting of a potted piezo-ceramic ring [3]. This transducer is a viable option to the proposed system due to its low cost and power requirements in comparison to commercial off-the-shelf transducers. A custom transceiver was also designed for the original UCSD modem and is sufficient as a proof of concept for the proposed design [3]. Lastly, the main contribution of this thesis comes from the digital design of the proposed adaptive modem. This design is described in greater detail in the following subsection.

4.1.1. Digital Modem Design

In order to illustrate the adaptive nature of the modem, the following is an example of a simple point-to-point exchange between two nodes, A and B, where node A wishes to send data to node B. This example is based on the notion of channel reciprocity. First, node A will send a Request To Send (RTS) packet to node B. This packet will include a series of chirp signals that can be used for measuring the channel. Upon hearing the RTS packet, the receiver will calculate the multipath delay spread, doppler shift, and SNR via its channel estimation module and determine the ideal bit rate and modulation scheme with which to communicate. Node B will then send a Clear To Send (CTS) packet intended for node A. This CTS packet will include the desired parameters that node B would like to communicate with. Node B will adjust its parameters to the ones specified in the CTS packet, followed by node A once it has received the packet. Node A will then begin transmitting its data to node B. In order to ensure all nodes can communicate with each other, control packets like the RTS and CTS packets will always be transmitted at a set of known and robust parameters.

In order to explain how this point to point exchange would take place within the modem architecture, please refer to Figure 4.2. The Receiver (Data) and the Transmitter, represent the adaptive modules in that their modulation scheme and bit rate can be selected from a set of pre-defined choices. In this figure, one can see how the analog to digital (ADC) input is routed to the Channel Estimation, Receiver (Control), and Re-

ceiver (Data) modules in parallel. The channel estimation module is made up of three submodules used to calculate the three targeted channel characteristics; multipath delay spread, doppler shift, and SNR. The Receiver (Control) module is a receiver module that is always set to the control packet modulation scheme and bit rate. The Receiver (Data) module is the adaptive receiver module that can change its modulation scheme and bit rate according to the control signals from the processor. The processor will function as a State Machine, as pictured in Figure 4.3. The processor will transition between the transmit and receive modes based on whether or not it has sensor data to transmit. Referring back to Figure 4.2, the last module is the adaptive Transmitter module. This module represents the transmit functionality of the modem. When data is ready to be sent, the bitstream will be sent from the processor and modulated according to the specified modulation scheme and bit rate.

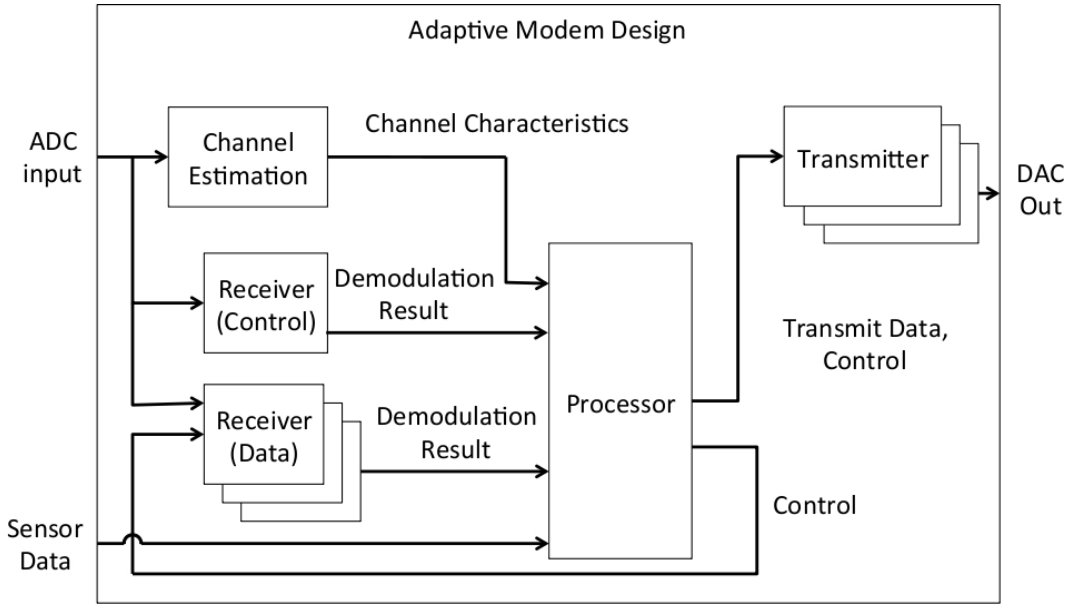

Figure 4.2: Adaptable Modem Block Diagram

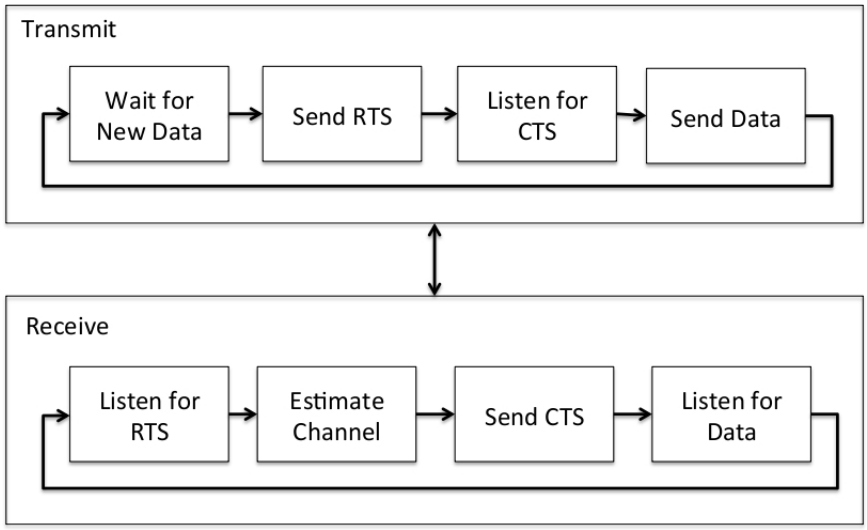

Figure 4.3: Processor State Machine

4.2. Simulation and Ocean Testing

We performed simulations and ocean tests in order to evaluate the plausibility and performance of the proposed adaptive modem. For these experiments, two modulation schemes were used; FSK and amplitude-modulated DSSS. These modulation schemes were chosen due to their potential in providing valuable information regarding the performance of different modulation schemes in different communication environments. The FSK transmitter and receiver is based on the UCSD modem in Dr. Bridget Benson's PhD Thesis [3] and is implemented in Verilog HDL. The DSSS transmitter and receiver is based on the UCSB AquaModem algorithm [22], which was discussed in the related works section and is implemented in Matlab.

We initially executed a set of simulations in order to find the best data rates for different links in a network and to understand the potential benefits of modifying data rates on a per link basis. We then performed ocean tests in order to evaluate the performance of the major components of the proposed adaptive modem in a real environment. The parameters for the Linear Frequency Modulated (LFM) Chirp, and FSK and DSSS modulation schemes used in both simulation and ocean tests are shown in Table 4.1.

The LFM Chirp was used for channel estimation, as described by Feng Tong et al. [24]. This LFM Chirp was also used for synchronization of DSSS packets, and both the LFM Chirp and a 15-bit reference Gold Code were used for synchronization of FSK packets.

Table 4.1: Chirp, FSK, and DSSS Signal Parameters

Chirp Signal Parameters		FSK and DSSS Signal Parameters	
Sweep Mode	up-chirp	FSK/DSSS carrier frequency	9kHz
Initial Frequency	8kHz	FSK/DSSS sampling frequency	192kHz
Maximum Frequency	12kHz	FSK space frequency	10kHz
Sweep Duration	50ms	FSK mark frequency	11kHz

4.2.1. Simulation Results

The simulation platform used in these experiments is an underwater acoustic propagation modeling software called the Acoustic Toolbox User interface and Post processor (AcTUP) [25]. This software allows the user to adjust the simulation environment in order to define attributes like bathymetric data, the positioning of the transmitting and receiving nodes, and the sound speed profile. Once the simulation environment is defined, AcTUP generates the amplitude and delay profile of the channel over the specified link. The AcTUP simulation environment was defined for five different transmitter and receiver pairs which were placed at different locations in the water column as shown in Figure 4.4. The amplitude and delay profiles for links 1 and 5 are shown in Figure 4.5. By looking at this figure, you can see that the two links have significantly different profiles. The multipath delay spread of link 5 is much shorter than that of link 1. However, link 5 has stronger individual multipath components than link 1. This reinforces the fact that different links in an underwater sensor network are likely to experience different channel characteristics.

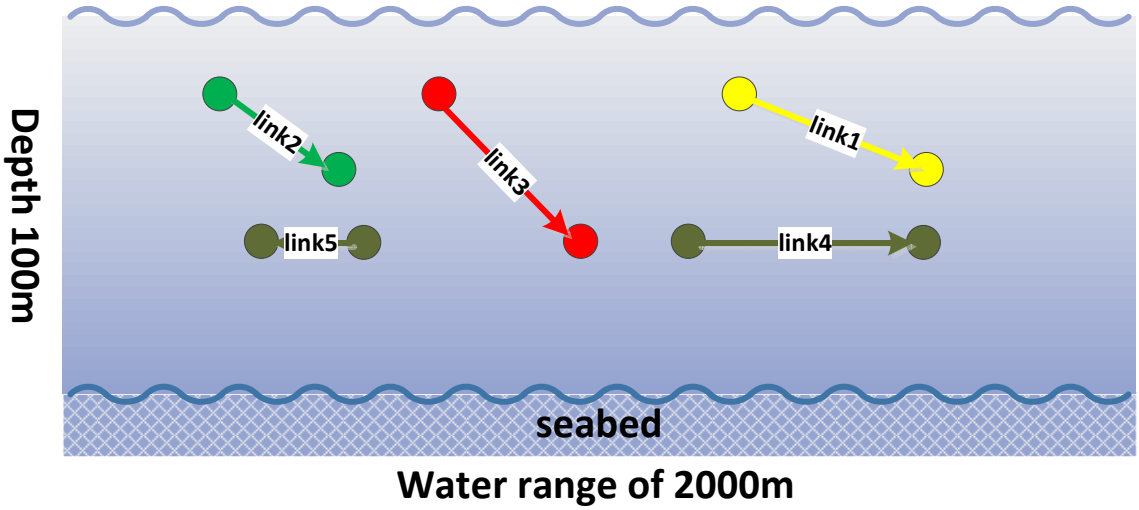

Figure 4.4: AcTUP Simulation Environment

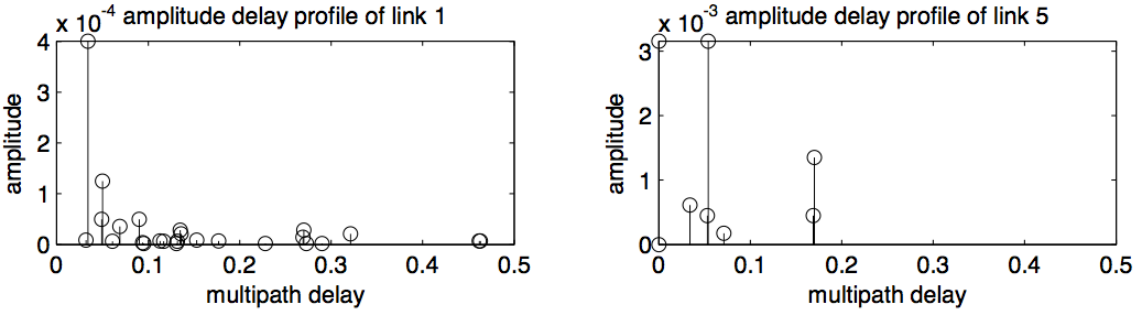

Figure 4.5: Multipath Amplitude and Delay Profile of Links 1 and 5

Once we collected the amplitude and delay profiles from AcTUP, we constructed a channel filter in Matlab for each link. Modulated data was then passed through the filters in order to simulate received data for each link. The simulated received data could then be demodulated and analyzed by calculating the bit error rate (BER) of the data. For each of these experiments, the simulation data consisted of 10 packets of 102 bits each. The demodulated data with the highest data rate whose BER was smaller than 10^{-2} was considered as the best rate for a specific link and modulation scheme. We chose 10^{-2} as our threshold because it represents the maximum tolerable BER for our purposes. The simulation results with the optimal data rates for each modulation scheme over each link are shown in Table 4.2.

Table 4.2: Optimal Data Rates For Simulated Channel Links

AcTUP Setup Parameters (m)				Data Rate (bps)	
Link	Tx depth	Rx depth	Distance	FSK	DSSS
1	20	40	200	200	1900
2	20	40	150	400	1900
3	20	60	200	100	1900
4	60	60	200	300	600
5	60	60	50	40	800

Though the optimal data rates in these tests are higher for DSSS when compared with FSK, this is not an indication of better performance of a particular modulation scheme, mainly due to the difference in implementation platforms. The DSSS Matlab implementation has much better data precision and higher order filters than the FSK Verilog implementation. This implementation difference is simply due to the fact that the Matlab implementation was not designed with the available resources of a specific embedded device in mind. A better analysis of the results would involve looking at the performace of each modulation scheme individually.

Taking the above explanation into consideration, the results show that the optimal data rate varies for each of the different links. These optimal data rates change from 40 bps to 400 bps for FSK, and from 600 bps to 1900 bps for DSSS. The results also show that rate adaptation can save considerable energy. For example, in the case of FSK modulated transmissions, if we consider the optimal fixed data rate that allows reliable communication under the worst channel conditions, all the links must communicate at 40 bps. The total energy consumed for all 5 links transmitting one bit at 40 bps is $0.125 * P_t$, where P_t is the transmitting power. Alternatively if the nodes perform rate adaptation and communicate at their optimal data rate, the total energy consumed is $0.0458 * P_t$. Therefore, if rate adaptation were used in this simulation environment, an energy saving of 63.4% could be achieved. Similarly, an energy saving of 45.8% could be achieved through rate adaptation in this simulation for DSSS modulated packets. As an additional benefit, faster data rates decrease the network's total congestion, and therefore decrease the probability of collisions, which, depending on the network's MAC protocol, can lead to a reduction in retransmissions and power. These results reinforce the initial motivations for the use of an adaptive modem in underwater sensor networks.

4.2.2. Ocean Test Results

In order to evaluate the performance of the major components of the proposed adaptive modem in a more realistic environment, we carried out experiments off the coast of San Diego, California in May 2011. In addition to analyzing the performance of modulation scheme and bit rate combinations, the chirp signal described in Table 4.1 and a 15-bit FSK-modulated gold code were evaluated for their effectiveness in packet synchronization.

The deployment setup is shown in Figure 4.6. The transmitter was hanging off the UC San Diego Scripps Pier, as pictured by the red transmitter pin, approximately 20 feet below the water surface in 25 feet of water. The receiver was attached to the hull of

a boat. Transmissions were received at two different sites, marked by yellow pins and labeled as Site 1 and Site 2. Site 1 and Site 2 are 265m and 638m from the transmitter, respectively. For each site, we transmitted FSK and DSSS data at six different data rates. For each of these data rates, we transmitted 20 packets with 102 bits each.

Figure 4.6: Map of Ocean Test Sites

After performing analysis on the received signals, it was clear that the chirp signal had better synchronization performance when compared to the Gold code. While the chirp was able to successfully synchronize with the start of the data sequence for all data packets, the Gold code only synchronized successfully with 68% of the packets at Site 1 and 70% of the packets at Site 2. This indicates that the chirp is a good candidate for channel estimation as well as symbol synchronization. This is an important finding to keep in mind when designing future transmitter and receiver pairs with different modulation schemes.

The BERs for FSK and DSSS modulated data were calculated with the chirp signal used for packet synchronization. Again, the purpose of these tests were not to compare the performance of FSK versus DSSS, since the differences in their implementation does not lend to a fair comparison, but to analyze their performance at different

Table 4.3: Ocean Test BERs for Site1/Site2

Data Rate	BER for FSK (%)	BER for DSSS (%)
50	9.67 / 7.99	0.22 / 2.36
100	19.33 / 16.62	1.47 / 1.86
200	12.58 / 27.39	1.53 / 6.40
300	21.86 / 27.78	0.78 / 7.07
400	21.67 / 31.75	3.56 / 13.58
500	35.26 / 40.60	16.97 / 32.30

bit rates. The results are summarized in Table 4.3. As shown, the BER increases with the data rate. This is most likely due to inter-symbol interference and ambient noise occurring within the frequency band, possibly caused by surface movement. The results also show that the average BER at Site 2 is higher than that at Site 1. To explain this, the channel for both sites, as shown in Figure 4.7, was measured. The figure shows that the Doppler shift and the multipath delay spread are both higher for Site 2 compared to Site 1. These ocean test results correspond with the AcTUP simulation results in the sense that BER varies significantly with both the data rate as well as the channel characteristics between the sender and receiver.

The ocean tests and simulations described in this chapter help motivate the need for a real-time adaptive underwater acoustic modem. We can see from the simulation and ocean test data that the two modulation schemes react differently to the channel conditions across different bit rates. We have also shown that having an adaptive bit rate has the potential to save power consumption through reduced transmission time.

The text of this chapter is, in part, based on the material as it appears in "Designing an Adaptive Acoustic Modem for Underwater Sensor Networks", IEEE Embedded Systems Letters, vol. 3, issue 3, December 2011. The thesis author was a co-primary researcher and author (with Lingjuan Wu). The other co-authors listed on this publication

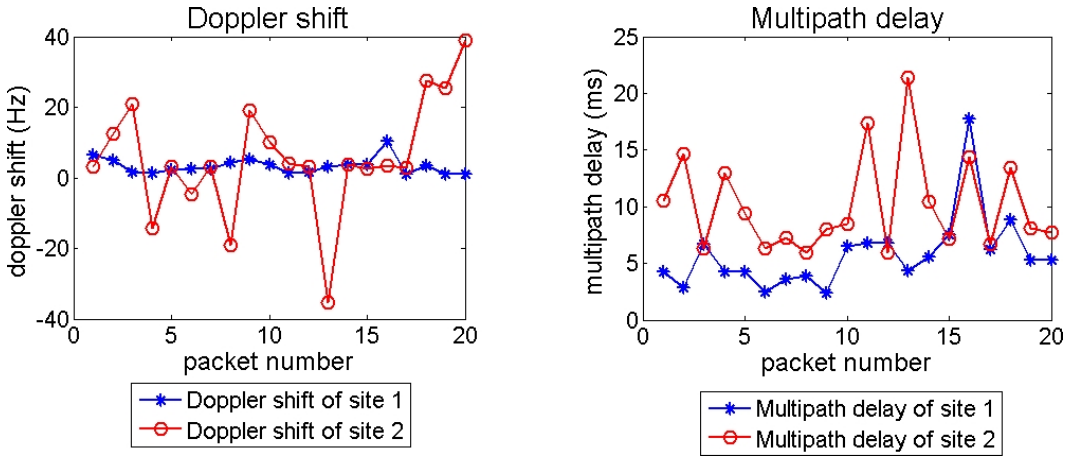

Figure 4.7: Ocean Test Channel Characteristics

[1] directed and supervised the research which forms the basis for this chapter.

Chapter 5.

Implementation

We implemented the transmitter and receiver portions of the proposed modem on a field programmable gate array (FPGA) in order to provide a test platform for different communication techniques. This test platform was designed for in-air transmissions in order to simplify the testing environment and allow for rapid prototyping of communication protocols. Ideally, this platform can be used to test implementations of different modulation schemes, and will eventually support the integration of additional modules such as the channel estimation module.

The ZedBoard [26] was selected as the hardware device for the test platform. We then connected the Chilipepper FPGA mezzanine card (FMC), developed by Toyon [27], to the ZedBoard via the ZedBoard's FMC header and used it as a radio-frequency front end for our design. As a sample modulation scheme, we chose to implement the FSK transmitter and receiver used in the ocean tests on our test platform. Once the implementation was completed, the test platform could successfully transmit data between two boards at a user-specified bit rate. Currently bit rates of 200bps and 400bps are supported.

The rest of this chapter is outlined as follows. Section 5.1 describes the specifications of the ZedBoard and Chilipepper FMC as well as the high level system design of the test platform. Section 5.2 goes into detail about the implementation of the FSK

Figure 5.1: ZedBoard

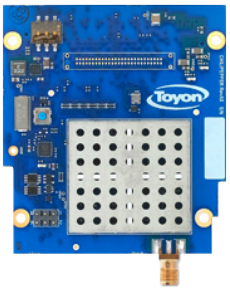

Figure 5.2: Toyon Chilipepper FMC

transmitter and receiver, and Section 5.3 describes the Matlab implementation of the channel estimation module.

5.1. Development Platform

We analyzed a number of boards in order to select an appropriate test platform for the proposed modem. The ZedBoard was chosen due to its state-of-the-art Xilinx Zynq 7020 All Programable SoC, and its ability to integrate with the necessary peripherals. Detailed specifications of the ZedBoard are shown in Table 5.1. The Chilipepper FMC is one of the recommended radio frequency front ends for the ZedBoard, and the majority of labs and tutorials for the Chilipepper FMC are integrated with the ZedBoard. The two boards are pictured in Figures 5.1 and 5.2.

The Chilipepper FMC seamlessly connects to the ZedBoard's FMC header. This FMC is a radio front end meant for rapid prototyping of physical layer waveforms. The main chip on the Chilipepper FMC is the Lime Microsystems RF-IC. It supports Multi-band operation, including full duplex operation around 2.1 GHz, time duplex in the 2.4 GHz band, broadband reception for waveforms such as GPS, and a modifiable design to accommodate frequencies in a range of UHF, L-band, and S-bands. In addition, the board hosts an onboard MCU to handle calibration and configuration tasks. The Chilipepper FMC also includes a standard SMA antenna connector.

A block diagram of the entire testing platform is shown in Figure 5.3. In order for

Table 5.1: ZedBoard Specifications

Processor	Dual ARM Cortex-A9 MPCore
	Up to 667 MHz operation
	NEON Processing / FPU Engines
Memory	512 MB DDR3 memory
	256 Mb Quad SPI Flash
	SD/MMC card cage
Connectivity	10/100/1000 Ethernet
	USB OTG and UART
Expansion	FMC (Low Pin Count)
	5 Pmod headers
Video/Display	HDMI output (1080p60 + audio)
	VGA connector
	128 x 32 OLED
	9 User LEDs
User Inputs	8 Slide switches
	7 Push button switches
Audio	24-bit stereo audio CODEC
	Stereo line in/out
	Microphone input and Headphone
Analog	Xilinx XADC header
	Supports 4 analog inputs
	2 Differential / 4 Single-ended
Debug/Programming	On-board USB JTAG programming port
	ARM Debug Access Port (DAP)
Power	12V DC input @ 3.0 A (max)
Dimensions	6.3 inches x 5.3 inches

the Chilipepper FMC to interface with the FPGA and ARM Processor on the ZedBoard, drivers for the FMC's microcontroller (MCU), digital-to-analog converter (DAC), and analog-to-digital converter (ADC) must be added to the hardware design on the ZedBoard. In addition, there are a number of different clock domains utilized in this design. These different clock domains are necessary in order to preserve the sampling frequency and carrier frequencies of the FSK transmitter and receiver, while meeting the requirements of the Chilipepper FMC. It is important to preserve these frequencies on the FSK transmitter and receiver, because the end goal is to use those blocks in an actual underwater modem. Therefore, this testing platform should act as a shell in which underwater modem modules can be easily swapped in and out, without needing to make significant changes. The functions of each module are described in the next few paragraphs. Please note that all analog-to-digital and digital-to-analog conversions happen on the Chilipepper FMC. Therefore, any modulated inputs or outputs at the FMC-ZedBoard interface are the digital representations of the desired analog signal.

We designed a software application for the ARM processor in order to send control signals to the FPGA and to send or receive a user-specified message. When a message is ready to be sent, its binary representation is written to the tx data register. All control signals, such as enabling or disabling the transmitter or receiver and controlling the bit rate, are written to the control register.

When the FSK transmitter module is enabled, it reads the user-specified message from the tx data register and modulates it. The modulated signal is sampled at 192KHz with a carrier frequency of 41-42KHz. These characteristics are optimized for use with the transducer that will be used in the proposed modem. The Chilipepper FMC requires two modulated inputs, I and Q. These two signals are identical except for a 90 degree phase shift. Consequently, the FSK transmitter generates its modulated signal from both a sine wave and a cosine wave. These two modulated signals, I and Q, are then sent to the digital up converter module for further processing. The FSK transmitter is described in greater detail in the next section.

The digital up converter module is necessary in up sampling and up converting

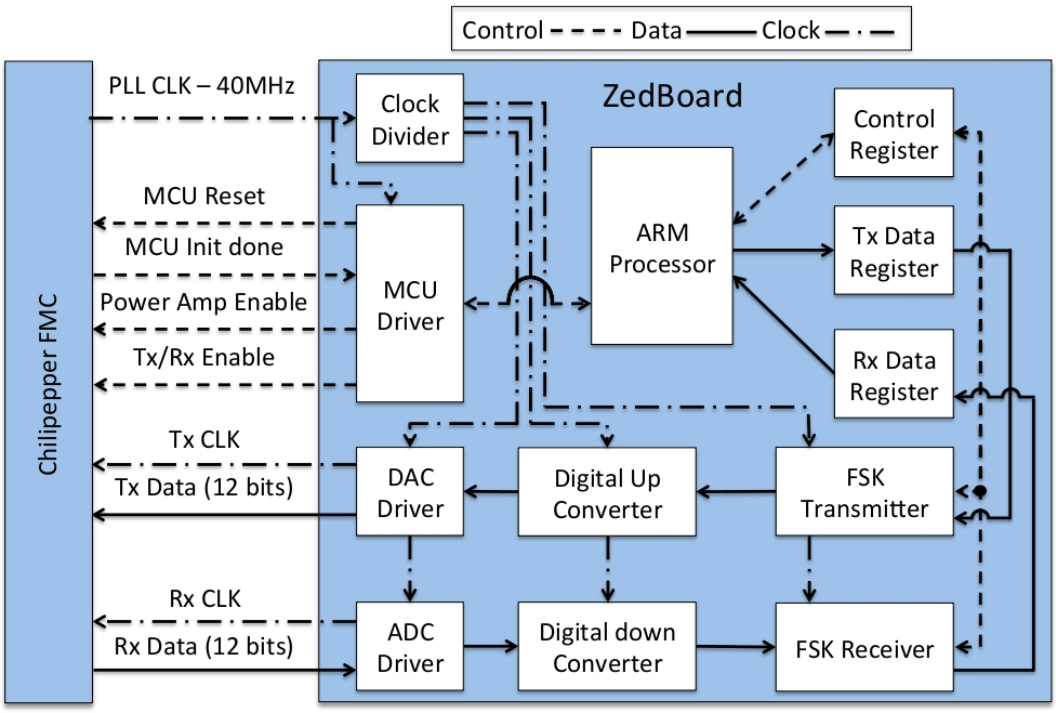

Figure 5.3: Development Platform Block Diagram

the two modulated signals from the FSK transmitter. The Chilipepper FMC supports modulated baseband signals between 750KHz and 20MHz. In order to meet these specifications, this module up samples the signals from 192KHz to 19.2MHz and up converts the signals from 40KHz to 800KHz. Up sampling is performed using a cascaded integrator-comb (CIC) Filter. The up conversion is done by multiplying the modulated signals with a 760KHz sine wave, and passing the product through a high pass filter.

The DAC driver interleaves the I and Q data signals from the digital up converter in order to conserve pins at the FMC interface. As a result, this module must be clocked at a rate of 2x the sample rate of the modulated input. In this case, I and Q are sampled at 19.2MHz, which requires the DAC driver to be clocked at 38.4MHz. This driver is responsible for sending the digital baseband modulated signals and transmit clock from the ZedBoard to the FMC.

The ADC driver is also clocked at 38.4MHz to match the sampling frequency of the digital modulated signals coming from the Chilipepper FMC. This driver separates the interleaved I and Q modulated signals and passes them to the digital down converter for further processing.

The digital down converter module is responsible for down converting and down-sampling the received signal back to the original requirements of the FSK receiver. Since the FSK receiver only requires one modulated signal for demodulation, the Q signal is discarded at this point. Similar to the digital up converter, the down conversion is done by multiplying the input modulated signal with a 760KHz sine wave, and passing the product through a low pass filter. The down sampling is again performed using a CIC filter.

The FSK receiver receives a modulated signal as input from the digital down converter module. When a packet is detected, it synchronizes with the packet and demodulates the data. The demodulated data is then written to the rx data register for the ARM processor to read. The FSK receiver is described in greater detail in the next section.

When the test platform is in receive mode and it has detected a packet, the re-

ceived message is written to the rx data register and a control signal is set to indicate that a message has been received. The software application will then read the message from the register and print it to the console for the user to see.

The MCU driver is clocked at 40MHz and allows the ARM processor to pass control signals to and from the MCU on the Chilipepper FMC. These control signals are responsible for status communication and enabling/disabling the receiver and transmitter on the FMC.

The clock divider module generates each of the necessary clocks from a 40MHz PLL reference clock provided by the Chilipepper FMC. It generates a 38.4MHz clock for the DAC and ADC drivers, a 19.2MHz clock for the digital up converter and digital down converter modules, and two clocks, 192KHz and 16KHz, for the FSK transmitter and receiver.

Now that the basic functionalities of the modules that make up the test platform have been explained, the next section will go into detail about the implementation of the FSK transmitter and receiver.

5.2. FSK Transmitter and Receiver Design

The FSK transmitter and receiver implemented on this test platform are originally based on the FSK transmitter and receiver from Dr. Bridget Benson's Thesis [3]. Modifications have been made to the original Verilog code in order to dynamically change the bit rate of the modem. This FSK transmitter and receiver pair use binary FSK with a carrier frequency of 40KHz. The mark, a binary 1, and space, a binary 0, frequencies are 42KHz and 41KHz respectively. An example of how the FSK transmitter would modulate a bit stream is shown in Figure 5.4. The implementation of the transmitter and receiver are described in the next sections.

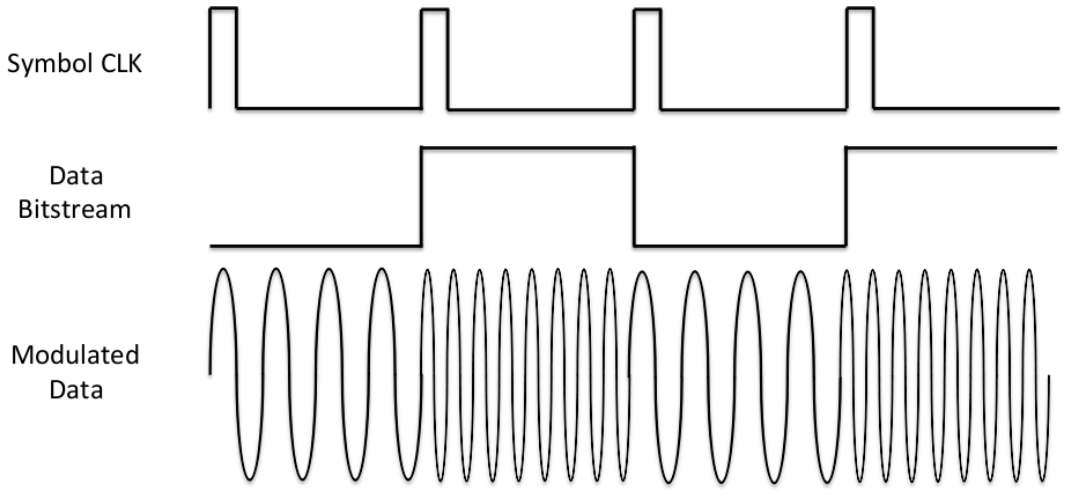

Figure 5.4: Binary FSK Modulation Example

5.2.1. FSK Transmitter

A block diagram of the FSK transmitter is shown in Figure 5.5. The transmitter has three main modules; Carrier Generator, Modulator, and Sin/Cos Generator. The FSK transmitter requires an enable signal and a data bitstream as inputs, and outputs the corresponding modulated data. One small change that was made to the original FSK transmitter in order to make it compatible with the test platform is the addition of a second modulated data output in order to generate both the I and Q signals discussed in the previous section.

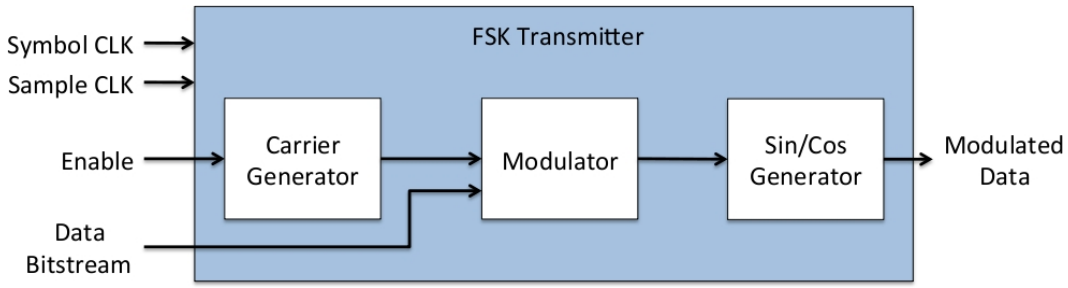

Figure 5.5: FSK Transmitter Block Diagram

The transmitter requires two clocks; a symbol clock and a sample clock. The symbol clock has a period equal to the specified bit rate. This clock is predominantly used by the modulator module and is aligned with the data bitstream to indicate when the next bit has arrived. The sample clock has a period equal to the sample rate of the modem. In this case, the sample rate is fixed to 192KHz. This rate was chosen in the original design as part of a hardware restriction for a data acquisition device. Since the rate is sufficiently fast according to the Nyquist Sampling Theorem, the sample rate was not changed.

The carrier generator module is in charge of generating the mark and space theta values that are used to construct the sinusoid used in FSK modulation. Both of these theta values are passed to the modulator block which outputs the correct mark or space theta value that matches with the binary 1 or 0 coming from the data bitstream. This final theta value is sent to the sine/cosine generator module which largely consists of a sine and cosine lookup table, matching the theta value to the actual sine/cosine signal value. The output of this module is the modulated data that will be sent to the digital up converter module for further processing.

5.2.2. FSK Receiver

A block diagram of the FSK receiver is shown in Figure 5.6. The receiver has five main modules; down converter, sync shaper, sync correlator, sync aligner, and FSK demodulator. It takes as input the received signal from the Chilipepper FMC, called rx data. The receiver outputs the final demodulated data as a binary bitstream. Packet synchronization is done by aligning the incoming packet with a known 15 bit gold code which is present in the packet header.

The receiver requires three clocks; a 4x symbol clock, a sample clock and a baseband sample clock. The rate of the 4x symbol clock is four times as fast as the symbol clock from the FSK transmitter. The sample clock is the same 192KHz clock that is connected to the FSK transmitter. This clock is only connected to the down

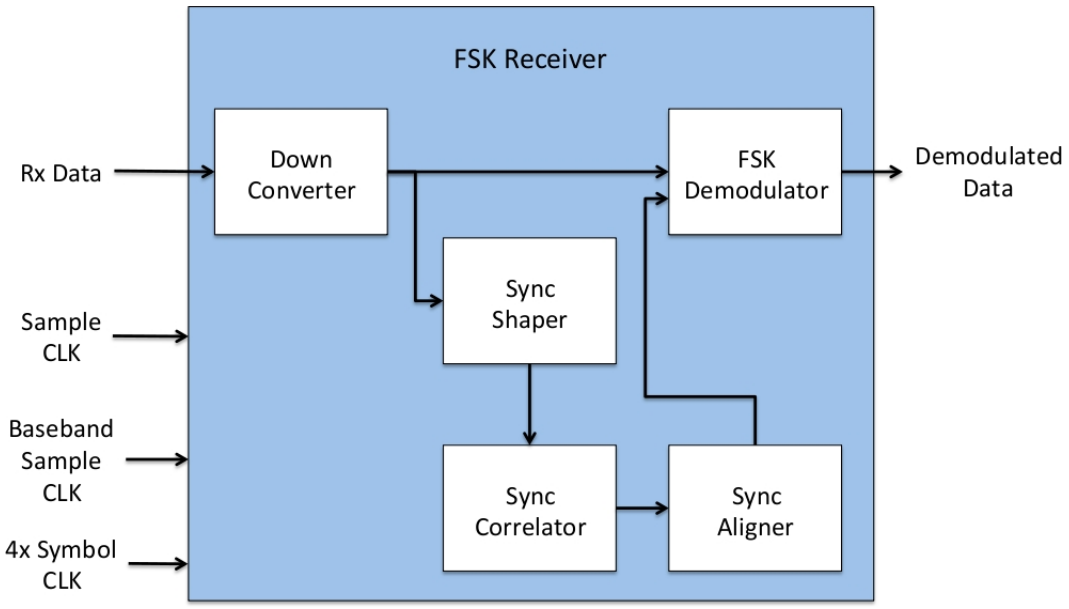

Figure 5.6: FSK Receiver Block Diagram

converter module. The rest of the modules in the receiver are clocked by the baseband sample clock. This clock has a period of 16KHz. These modules are clocked at a slower rate because the output of the down converter is a 0-5KHz signal, and a slower processing clock rate is more suitable. The individual modules of the FSK receiver are described below.

The down converter module down converts the rx data signal by multiplying the signal with a continuous 40KHz signal generated from a cosine lookup table and then passing the product through a 5KHz low pass filter. The mark and space frequencies will then be represented by 2KHz and 1KHz signals respectively. These signals are re-sampled at the rate of the baseband sample clock. This down converted and down sampled rx data signal is then passed to both the FSK demodulator and the sync shaper for further processing.

The sync shaper module shapes the baseband rx data signal into a square-like waveform. This is done by first passing the baseband rx data signal through both a 1KHz and a 2KHz band pass filter in parallel. The absolute values of the outputs of each

of the band pass filters are summed over one period of the 4x symbol clock. The 1KHz band pass filter sum is then subtracted from the 2KHz band pass filter sum which results in either a positive or negative value. In this case, a positive value would represent a binary 1 and a negative value would represent a binary 0. This difference result is then passed to the sync correlator for further processing.

The sync correlator module essentially correlates the difference result from the sync shaper module with the 15-bit gold code used for packet synchronization. This is done with a 60-bit shift register that acts as a sliding window for the difference result. It is 60 bits wide because the window must cover the length of the 15-bit gold code. Since the difference result is sampled at four times a symbol period, the 15-bit gold code must also be oversampled by 4. This results in a 60-sample gold code. The cross-correlation between the difference result and the gold code is calculated for one window period and the result is sent to the sync aligner to search for correlation peaks. In parallel, the orthogonal correlation is also calculated by finding the cross-correlation with the difference result and a 15-bit gold code that is orthogonal to the reference gold code, in the same manner. This orthogonal correlation is used as a dynamic threshold in the sync aligner module.

The sync aligner module aligns the incoming packet with the highest peak in a a two-window sized period. This detection period begins when the first peak occurs above the dynamic threshold. This two-window alignment period is necessary in order to avoid finding false peaks if the data within the packet has a high correlation with the gold code. Once the highest peak has been found, this index is sent to the FSK demodulator module, along with a synchronized symbol clock which is generated from the 4x symbol clock.

The FSK demodulator block demodulates the baseband rx data signal into binary 1s and 0s which are output as the demodulated data and sent to the ARM processor. This process is implemented as a classic matched filter demodulator. The rx data signal is passed through another set of 1KHz and 2KHz band pass filters in parallel. The output of each of the band pass filters is squared and summed over a period of one symbol.

If the resulting product of the 1KHz band pass filter is larger than the 2KHz band pass filter, then the demodulated bit is a binary 0. Otherwise, the demodulated bit is a binary 1.

The modules described in this section make up the FSK receiver which includes gold code synchronization and demodulation. The FSK transmitter, along with all its modules, was described in the previous section. This concludes the description of the modules implemented on the ZedBoard as part of the test platform. The next section describes the channel estimation implementation in Matlab and how it can be integrated into the test platform in the future.

5.3. Channel Estimation

The channel estimation module for the proposed modem has been implemented in Matlab. Although the module has not been implemented as part of the test platform at this point, the structure of the channel estimation code lends itself to a straight-forward hardware implementation. This task has been allocated to future work. This module is key in the design of the proposed modem in that it allows the modem to make decisions based on the current channel characteristics, and thus adapt its bit rate and modulation scheme in real time. Once this module is added to the ZedBoard design, the user will no longer need to specify a bit rate in order to demonstrate the adaptive capabilities of the modem. The Matlab implementation can be described as follows.

Upon receiving a series of chirp signals which have been included in a request-to-send (RTS) packet, as shown in Figure 5.7, the three sub modules within the channel estimation module will calculate the multipath delay spread, doppler shift, and SNR. These modules are described in detail below.

Multipath delay spread can be defined as the time between the arrival of the first significant path and the last multipath component. This delay spread is commonly calculated by finding the root mean squared (RMS) delay spread of the received signal [28]. For this implementation, the multipath delay spread is calculated by cross-correlating

the received chirp signal with the original chirp signal in order to generate an amplitude delay profile of the received chirp. The RMS of the amplitude delay profile is used as a threshold to differentiate strong multipath components from insignificant ones. The delay spread is then computed by calculating the time between the path with the maximum amplitude (usually the line of sight path) and the last path whose amplitude is greater than the RMS threshold.

Doppler shift is typically caused by ocean swells and relative motion between transmitting and receiving nodes. This shift results in a perceived shift in frequency at the receiving node. Doppler shift is relative to the frequency of the original signal and can be defined by $\hat{f} = \delta * f$ where $\hat{f}$ is the Doppler shift, δ is the Doppler scaling factor of the channel, and f is the carrier frequency of the transmitted signal. The Doppler scaling factor can be defined as $\delta = \tau_{rx}/\tau_{tx} - 1$, where τ represents the measured time between the start of two signals, or in this case chirps, as shown in Figure 5.7. Specifically, τ_{tx} is the time between the start of two chirps as defined by the packet header structure and sent by the transmitter, and τ_{rx} is the time between the start of two chirps as observed in the received packet header.

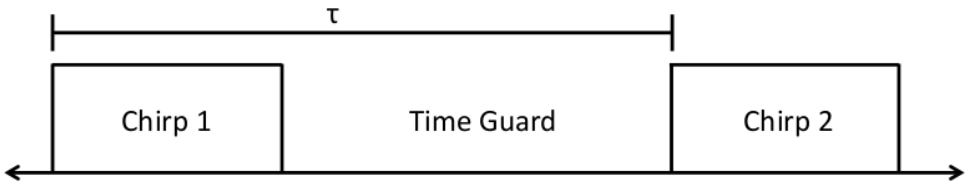

Figure 5.7: Packet Header Structure For Channel Estimation

SNR is a much simpler calculation and can be defined as:

$$snr = var(received\_signal)/var(ambient\_noise) \tag{5..1}$$

where the function $var(x)$ is the variance of x. Using the packet header structure from Figure 5.7, the variance of the ambient noise can be calculated during the time guard between the two chirps, and the variance of the signal can be calculated during the transmission of one of the chirps.

The channel characteristics that are estimated in these three channel estimation submodules can be used to select a modulation scheme and bit rate combination that is expected to perform well given the observed channel. Since the channel varies over time, this channel estimation processes will occur at the beginning of every series of data packets that will be sent across a link.

This concludes the explanation of the implementation of the test platform. This platform consists of a Chilipepper FMC (radio front end) and a ZedBoard (digital modem). The platform is intended for prototyping modulation schemes and bit rates intended for underwater communication in a real environment. Once the channel estimation module and an additional transmitter and receiver pair with a second example modulation scheme is added to the design, the test platform will be fully capable of demonstrating the adaptive capabilities of the proposed modem in real time. For now, the adaptive capabilities are restricted to a user-modified bit rate. The next section discusses the implementation results for this test platform.

5.4. Results

The results discussed in this section pertain to the test platform described throughout this chapter. The full design was implemented on a pair of ZedBoards, each connected to its own Chilipepper FMC. The device utilization for a single ZedBoard is shown in table 5.2. A brief description of the configurable logic resources on a Zynq 7020 SoC is provided below.

The FPGA portion of the Zync 7020 is composed of a number of configurable logic blocks (CLBs). Each CLB contains a pair of slices. Each slice is composed of four 6-input lookup tables (LUTs) and eight storage elements, or registers [29].

A DSP48E1 is a special type of logic element that supports common digital signal processing functions such as multiply, multiply accumulate, multiply add, barrel shift, bitwise logic functions...etc [29]. The majority of DSP48E1 slices that are used in this design are for the finite impulse response (FIR) and cascaded integrator-comb

(CIC) filters in the digital up converter and digital down converter modules.

A BUFG, or global clock buffer, is a high-fanout buffer that connects signals to the global routing resources on an FPGA. This resource is typically used for clock nets in order to minimize skew when distributing the signal [30].

RAMB18E1s and RAMB36E1s are 18Kb and 36Kb block RAMs respectively. Block RAMs on a Zynq 7020 SoC can store up to 36Kb of data and can be configured as either two independent 18Kb RAMs or one 36Kb RAM [31].

Since the utilization of each of these resource types is generally below 50%, it is possible to implement additional modules like channel estimation and a second modulation scheme on the device.

Table 5.2: Device Utilization

Resource Type	No. Resources Used	No. Resources Available	% Utilization
BUFG	13	32	40
DSP48E1	60	220	27
RAMB18E1	8	280	2
RAMB36E1	34	140	24
Slice	7140	13300	53
Slice Register	11299	106400	10
Slice LUT	21375	53200	40

In order to evaluate the FSK transmitter and receiver on this test platform, we sent data packets from one board and received them on another. Each packet consisted of a 32-bit header followed by 200 bits of data. For each test scenario, approximately 25 packets were sent and received. Two different bit rates were tested; 200 bits per second (bps) and 400 bps. The results of these tests are shown in Table 5.3.

The first column, titled Communication Method, refers to the method in which packets were transmitted from one board to the other. The two methods that were used in

our experiments are transmission via cable and antenna. The cable method involves simply unscrewing the antennas on the Chilipepper FMCs and connecting the two boards with an SMA cable. We initially tested the boards with the cable method in order to observe performance with minimal noise interference. However, the boards are not sufficiently shielded for this type of test, and we saw no significant difference in noise interference between the two methods. Alternatively, we did observe an increase in power of the transmitted signal during cable mode transmissions, which resulted in a higher SNR.

Table 5.3: Test Results

Note: Sync offset indicates how close the receiver was from aligning with the actual start of the packet, measured in bits. A negative sync offset occurs when the receiver aligned after the start of the packet and a positive sync offset occurs when the receiver aligned before.

Comm. Method	Bit Rate (bps)	Sync Rate (%)	Sync Offset Mode (% occurrence)	Avg. Sync Offset (bits)	BER (%)
Cable	200	0	16 (46%)	15	11.44
Antenna	200	12.5	-1 (15%)	5	15.48
Cable	400	40	0 (40%)	7	9.23
Antenna	400	8	-1 (32%)	6	10.87

In these experiments, we also tested the performance of 15-bit gold code synchronization for our FSK transmitter and receiver design. Overall, the synchronization performance was poor. These results are also shown in Table 5.3. The sync rate refers to the number of packets that were synced correctly divided by the number of packets that were sent. We added a feature in software that aligns the received bitstream with the expected bitstream according to the best fit. The synchronization offset is then calculated as the offset in bits of the actual alignment from the best-fit alignment. The mathematical mode and the average of this sync offset is shown in the table. For reference, the rate of occurrence of the mode is included as well. The bit error rate (BER) is calculated

according to the best-fit alignment for all packets that were received.

As expected, the cable method shows a lower BER in comparison to the antenna method. This statistic is most likely a result of the difference in SNR between the two methods. The signal strength discrepancy can be seen in Figure 5.8 by looking at the difference in amplitude between the two signals, once most of the noise has been filtered away. These figures show close to a 100x increase in signal strength from the antenna mode to the cable mode. These signals were captured using Chipscope during the transmission of a packet sent at 200bps. As a point of reference, Figure 5.9 shows the ideal output of the receiver's low pass filter (LPF) for both a binary 1 and a binary 0.

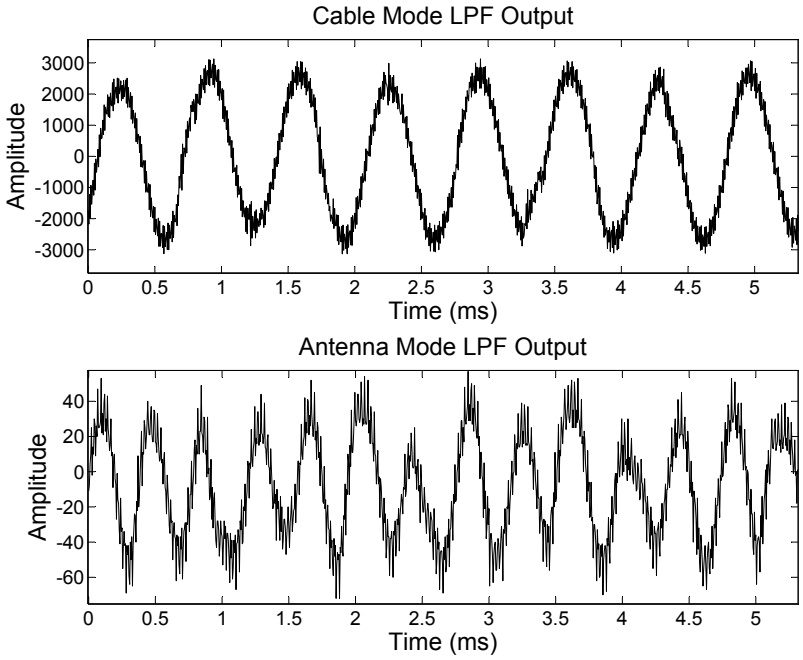

Figure 5.8: LPF Output of Received Signal for Antenna and Cable Modes

Note: These graphs show a small window of the actual received signal. The signal should be either a 1KHz or 2KHz sine wave, representing a binary 0 or 1 respectively. Since the captured window is not synchronized with the incoming signal, a resulting sine wave with a frequency somewhere between 1KHz and 2KHz is possible if the window falls during a transition between bits.

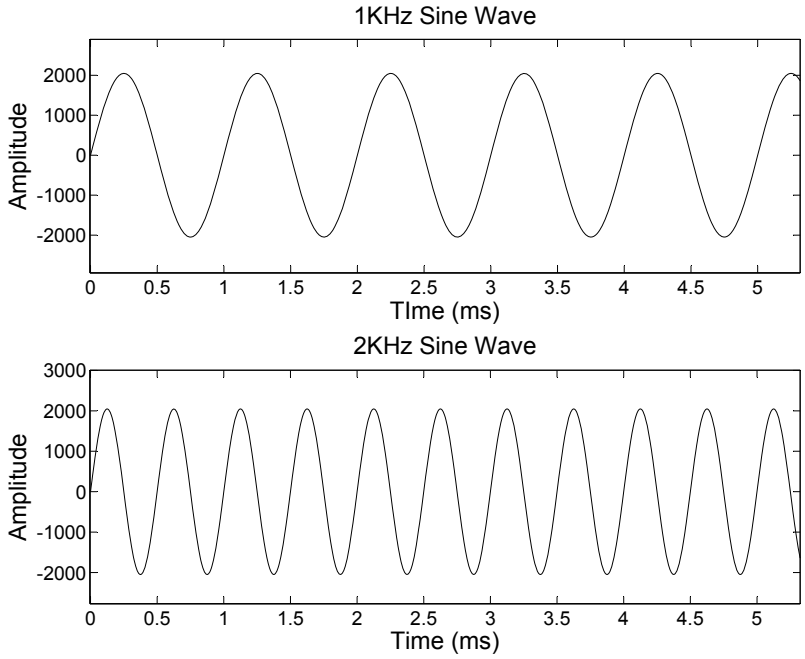

Figure 5.9: 1KHz and 2KHz Generated Sine Waves

Note: These figures portray an ideal output from the FSK receiver's LPF, in which a 1KHz sine wave represents a binary 0 and a 2KHz sine wave represents a binary 1.

The results also indicate that packets transmitted at 400bps have a slightly lower BER when compared with packets transmitted at 200bps. This difference in BER is most likely attributed to alignment resolution. If you recall from the description of the sync correlator module in the FSK receiver discussed in Section 5.2.2, the 60-bit shift register that is used for cross correlation with the gold code samples the shaped signal at 4 times the symbol period. Therefore, our sampling rate for the sync correlator module increases with the bit rate. This characteristic translates to faster bit rates having a higher alignment resolution when compared with slower bit rates. Since 400bps is 2x faster than 200bps, it will have 2 times the alignment resolution, resulting in a potentially more accurate alignment and a higher probability of having a lower BER when compared with packets transmitted at 200bps.

Now that we've concluded analyzing the BERs for each of the experiments, we will now move on to discuss the performance of the 15-bit gold code synchronization. Figure 5.10 shows the sync offsets for every packet that was received in each of the experiments. The alignment resolution issue discussed in the previous paragraph will also have an effect on the sync offset. The higher the alignment resolution, the more accurate the correlation result will be. This condition most likely explains the increase in sync rate between the experiments using the cable method with bit rates of 200bps and 400bps.

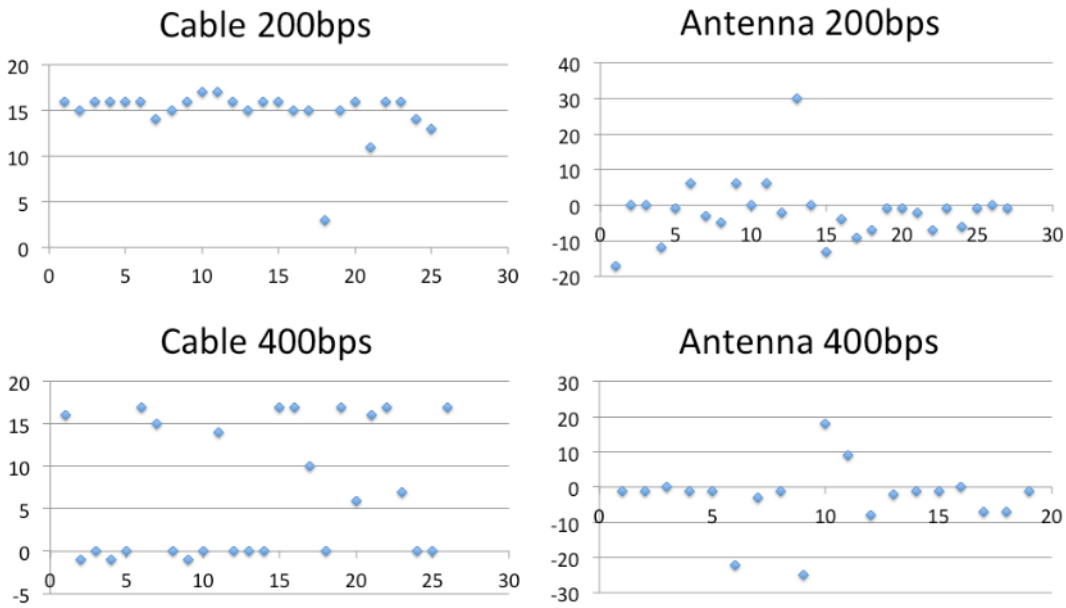

Figure 5.10: Sync Offset

One notable characteristic of the test results for both cable experiments is that a majority of the sync offsets are divided between 0 and 16. Specifically, 80% of the sync offsets in the cable method test with a bit rate of 200bps are between 15 and 17, with 46% of the sync offsets equal to 16. If the sync offset is 16 bits, the highest correlation peak would have occurred at bit 16 of the packet header. For these tests, the packet header consisted of 15 bits of zero-padding, 15 bits of gold code, and 2 additional bits of zero-padding. The correlation shift register will be full of the modulated equivalent of

binary 0s by bit 15 of the packet header. It is possible that since the alignment resolution is so poor for the 200bps case that the Sync Correlator module is simply finding a peak when any modulated signal has filled the shift register. For the case of the 400bps test, 40% of the packets aligned correctly, and 35% of the packets had a sync offset between 15 and 17. These results may show a correlation with the improved alignment resolution (over the 200bps case).

The two antenna test cases are also subject to the same alignment resolution characteristics. However, the results show a decrease in sync rate from the 200bps case to the 400bps case. Since the antenna transmission method results in a lower SNR, it is possible that the correlation result at the 15th bit of the packet header (the point at which the shift register fills) does not pass the peak threshold, and the chance of early alignment is reduced.

After analyzing the results in detail it is apparent that this particular implementation of 15-bit gold code synchronization is insufficient for proper communication. One way of improving the design would be to separate the synchronization module from the FSK receiver and implement a modulation-scheme and bit rate independent synchronization technique using the chirp signal described in section 4.2. This improvement would also have the benefit of saving implementation time and device resources since each modulation scheme would not need to implement its own synchronization module.

It is also important to note that the BERs are generally higher than desired for reliable communication. We can expect some improvement with a better synchronization technique. In addition, no attempts have been made to reduce the BER by using an error-correcting code. This issue of high BERs along with its solutions points out the need for such a test platform in identifying problems and making improvements to a digital underwater modem design. Therefore, we believe that this test platform will be useful in future prototyping of underwater modem protocols.

Chapter 6.

Conclusion

In this thesis I present my work on the design of an adaptable underwater acoustic modem and the implementation of a test platform for rapid prototyping of underwater modems in a real environment. I also discuss simulation and ocean test results that help show potential benefits of an adaptive modem through the theoretical possibility of reduced power consumption and increased robustness to the underwater communication channel.

The proposed adaptable modem will have the capability of measuring the communication channel and estimating a set of channel characteristics. These characteristics will be used to adapt the modulation scheme and bit rate of the modem in real time in order to improve reliability and power efficiency through optimized data rates. In addition, the components of the modem will be designed with cost in mind in order to ensure a low-cost device. The goal of this modem is to provide a cost-effective and improved solution to acoustic communication within underwater wireless sensor networks.

We conducted simulations in AcTUP across five different communication links. The results of these experiments show that the characteristics of the communication channel can change significantly depending on the location of the transmitting and receiving nodes. We also show how using an adaptive bit rate has the potential to reduce total power consumption while staying below a bit error rate (BER) threshold.

We performed ocean tests using two different modulation schemes, FSK and DSSS, across a range of different bit rates. The ocean tests confirm our findings from the simulations that channel characteristics can change depending on the location of the transmitting and receiving nodes, and that the BER is effected by both the bit rate and the changing channel characteristics.

The conclusions that we draw from these simulations and ocean tests support our hypothesis that an adaptable modem which can change its bit rate and modulation scheme depending on measured channel characteristics can be beneficial in underwater wireless sensor networks with mobile nodes in shallow water environments.

We also present our implementation of a test platform which is designed in such a way that modulator and demodulator modules can be rapidly prototyped and tested. Our implementation currently supports FSK modulation with modulated gold code synchronization and two bit rate options. Future improvements of the test platform, like the addition of a channel estimation module and a second modulation scheme, will allow for testing of the proposed adaptable modem design.

Bibliography

[1] L. Wu, J. Trezzo, D. Mirza, P. Roberts, J. Jaffe, Y. Wang, and R. Kastner, "Designing an adaptive acoustic modem for underwater sensor networks," *Embedded Systems Letters, IEEE*, vol. 4, no. 1, pp. 1–4, 2012.

[2] P. Roberts. (2009, July) Autonomous underwater explorer: Jaffe laboratory for underwater imaging. [Online]. Available: http://jaffeweb.ucsd.edu/node/81

[3] B. Benson, "Design of a low-cost underwater acoustic modem for short-range sensor networks," Ph.D. dissertation, The University of California, San Diego, 2010.

[4] A. Goldsmith, *Wireless Communications*. 40 West 20th Street, New York, NY: Cambridge University Press, 2005.

[5] M. Stojanovic, "On the relationship between capacity and distance in an underwater acoustic communication channel," *ACM SIGMOBILE Mobile Computing and Communications Review*, vol. 11, no. 4, pp. 34–43, 2007.

[6] I. F. Akyildiz, D. Pompili, and T. Melodia, "Challenges for efficient communication in underwater acoustic sensor networks," in *ACM SIGBED Review*, 2004.

[7] L. Freitag, M. Grund, S. Singh, J. Partan, P. Koski, and K. Ball, "The whoi micro-modem: An acoustic communications and navigation system for multiple platforms," in *IEEE Oceans Conference*, Washington, DC, 2005.

[8] J. Partan, J. Kurose, and B. N. Levine, "A survey of practical issues in underwater networks," *SIGMOBILE Mob. Comput. Commun. Rev.*, vol. 11, no. 4, pp. 23–33, Oct. 2007. [Online]. Available: http://doi.acm.org/10.1145/1347364.1347372

[9] B. Li, S. Zhou, M. Stojanovic, L. Freitag, and P. Willett, "Non-uniform doppler compensation for zero-padded ofdm over fast-varying underwater acoustic channels," in *IEEE Oceans 2007 - Europe*, Aberdeen, Scotland, June 2007.

[10] (2013, June) Aquamodem 1000 data sheet. Aquatec Group Limited. [Online]. Available: http://www.aquatecgroup.com/images/datasheets/aquamodem1000.pdf

[11] (2013, June) Linkquest underwater acoustic modems uwm2000h specifications. LinkQuest. [Online]. Available: http://www.link-quest.com/html/uwm2000h.htm

[12] (2013, June) S2c 48/78 underwater acoustic modem. EvoLogic. [Online]. Available: http://www.evologics.de/en/products/acoustics/s2cr_48_78.html

[13] (2013, June) Micron data modem - underwater acoustic modem. Tritech. [Online]. Available: http://www.tritech.co.uk/media/products/micron-data-modem.pdf

[14] (2013, June) Aquacomm: Underwater wireless modem. DSPComm. [Online]. Available: http://www.dspcomm.com/products_aquacomm.html

[15] (2013, June) Teledyne benthos smart products - sm-975. Teledyne Benthos. [Online]. Available: http://www.benthos.com/index.php/product/smart_products/sm-975

[16] (2013, June) Aquasent modem. AquaSeNT. [Online]. Available: http://www.aquasent.com/

[17] E. Gallimore, J. Partan, I. Vaughn, S. Singh, J. Shusta, and L. Freitag, "The whoi micromodem-2: A scalable system for acoustic communications and networking," in *OCEANS 2010*, 2010, pp. 1–7.

[18] S. Singh, S. Webster, L. Freitag, L. Whitcomb, K. Ball, J. Bailey, and C. Taylor, "Acoustic communication performance of the whoi micro-modem in sea trials of the nereus vehicle to 11,000 m depth," in *OCEANS 2009, MTS/IEEE Biloxi - Marine Technology for Our Future: Global and Local Challenges*, 2009, pp. 1–6.

[19] J.-H. Jeon, N.-Y. Yun, H. Nam, C.-G. Hong, S.-J. Park, S.-H. Park, S. An, C.-H. Kim, G.-H. Yang, and Y.-S. Ryuh, "A moving underwater communication system with bio-inspired fish robots," in *Proceedings of the Seventh ACM International Conference on Underwater Networks and Systems*, ser. WUWNet '12. New York, NY, USA: ACM, 2012, pp. 15:1–15:7. [Online]. Available: http://doi.acm.org/10.1145/2398936.2398956

[20] H. Yan, S. Zhou, Z. Shi, J.-H. Cui, L. Wan, J. Huang, and H. Zhou, "Dsp implementation of siso and mimo ofdm acoustic modems," in *OCEANS 2010 IEEE - Sydney*, 2010, pp. 1–6.

[21] P.-P. Beaujean, E. Carlson, J. Spruance, and D. Kriel, "Hermes - a high-speed acoustic modem for real-time transmission of uncompressed image and status transmission in port environment and very shallow water," in *OCEANS 2008*, 2008, pp. 1–9.

[22] R. A. Iltis, H. Lee, R. Kastner, D. Doonan, T. Fu, R. Moore, and M. Chin, "An underwater acoustic telemetry modem for eco-sensing," in *Oceans, 2005. Proceedings of MTS/IEEE*, Washington, DC, September 2005.

[23] A. Radosevic, T. Duman, J. Proakis, and M. Stojanovic, "Channel prediction for adaptive modulation in underwater acoustic communications," in *OCEANS, 2011 IEEE - Spain*, 2011, pp. 1–5.

[24] F. Tong, B. Benson, Y. Li, and R. Kastner, "Channel equalization based on data reuse lms algorithm for shallow water acoustic communication," *Sensor Networks, Ubiquitous, and Trustworthy Computing, International Conference on*, vol. 0, pp. 95–98, 2010.

[25] A. Maggi and A. Duncan. (2013, May) Centre for marine science and technology - underwater acoustic propagation modelling software - actup. [Online]. Available: http://cmst.curtin.edu.au/products/actoolbox.cfm

[26] (2013, June) Zedboard. [Online]. Available: http://www.zedboard.org

[27] (2013, June) Chilipepper fmc. Toyon. [Online]. Available: http://www.toyon.com/chilipepper.php

[28] H. Li, Z. Bi, D. Liu, J. Li, and P. Stoica, "Channel order and rms delay spread estimation for ac power line communications," in *Statistical Signal and Array Processing, 2000. Proceedings of the Tenth IEEE Workshop on*, 2000, pp. 229–233.

[29] (2013, August) 7 series fpgas configurable logic block user guide. Xilinx. [Online]. Available: http://www.xilinx.com/support/documentation/user_guides/ug474_7Series_CLB.pdf

[30] (2012, January) 7 series fpga libraries guide for hdl designs. Xilinx. [Online]. Available: http://www.xilinx.com/support/documentation/sw_manuals/xilinx13_4/7series_hdl.pdf

[31] (2012, October) 7 series fpgas memory resources user guide. Xilinx. [Online]. Available: http://www.xilinx.com/support/documentation/user_guides/ug473_7Series_Memory_Resources.pdf